

# Fault-tolerance thresholds for linear optical quantum computations

Chris Dawson, Henry Haselgrove, Michael Nielsen

PRL **96**, 020501 (2006) arXiv:quant-ph/0509060  
quant-ph/0601066



*Roughly speaking, our results show that scalable optical quantum computing is possible in the combined presence of both photon loss and depolarization noise (as a general proxy for all types of local noise other than loss), provided that the loss rate is less than  $3 \times 10^{-3}$  and the depolarization rate is less than  $10^{-4}$ .*

e.g. Y'all bin sufferin from kewbits depolarizin' ?

This talk is an elaboration of this statement:

- Basics of fault-tolerant quantum computation.
- Fault-tolerant quantum architectures and threshold estimates.
- Optical implementations of a fault-tolerant architecture.
- Results and conclusions.

## Introduction

*Goal of fault-tolerance*: design architectures for arbitrarily long quantum computations that can tolerate a certain level of noise before they start producing useless output.

Noise is considered in terms of *error models* that aim to capture the *effects* of noise on qubits, not the noise itself. This makes for simplified statements such as "A Pauli / loss error occurs with probability  $\epsilon$ ."

A fault-tolerance *threshold* expresses the maximum tolerable error rate in each physical primitive. A threshold serves as a measure of how good a fault-tolerant architecture is, and also as a target fidelity for gates and qubits *in arbitrarily large quantum computations*.

Thresholds are influenced by

- Error model (particularly error correlations)
- Geometric considerations
- The fault-tolerant architecture.

In a nutshell, fault-tolerant architectures aim to maximize thresholds whilst minimizing the overheads due to encoding and postselection.

## Basic fault-tolerance

Not concerned with making better gates and qubits, but with “building reliable devices from unreliable components.”

Reliability of qubits and gates can be improved via physical encoding, remaining errors are accepted as inevitable.

### Basic assumptions:

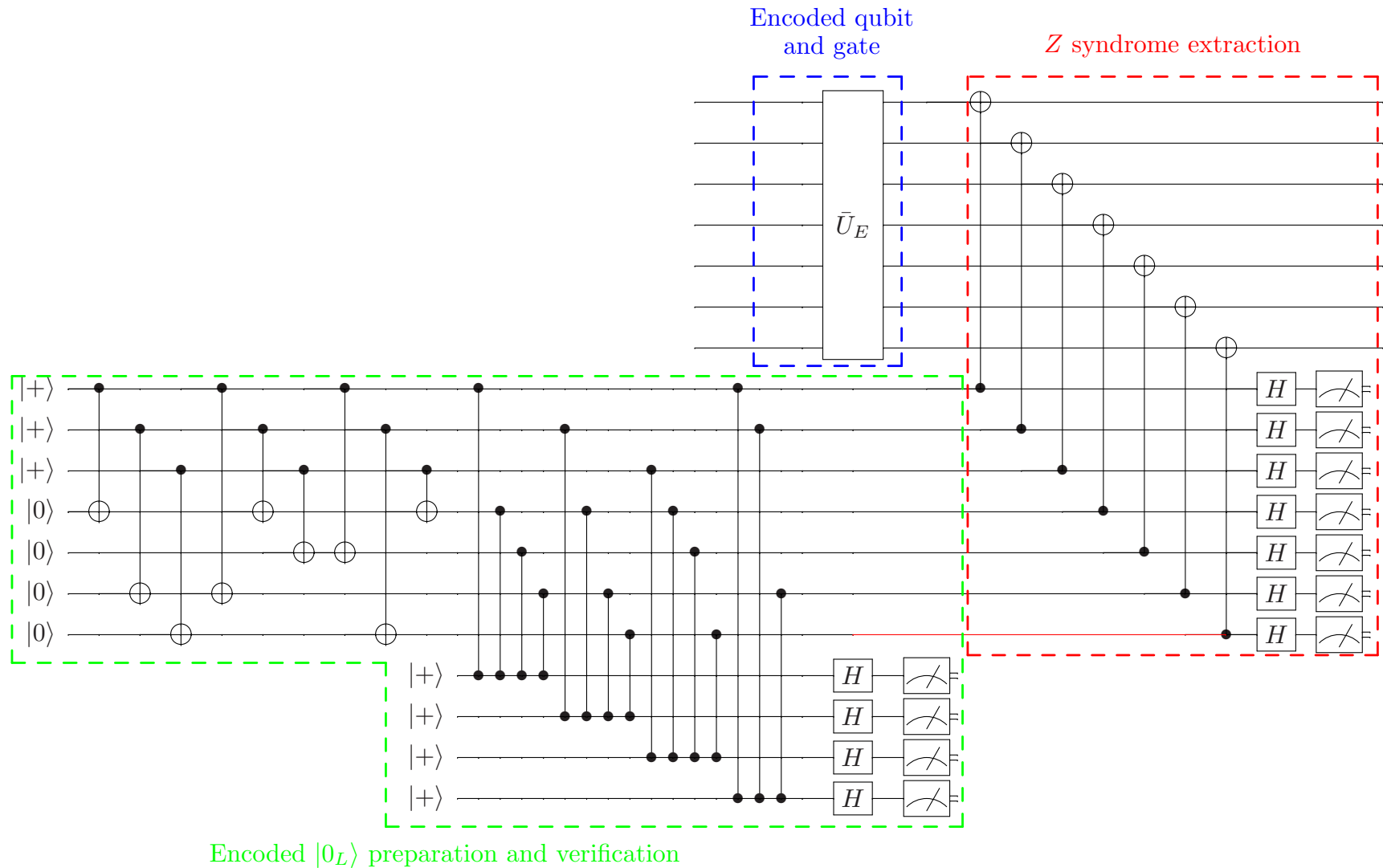
- Noise is “reasonable” i.e. not too non-local and not too non-Markovian.
- Operations can be applied in parallel (essential).
- Supply of pure or nearly pure ancilla qubits (also essential).

### Basic principles:

- Qubits and gates are *encoded* using a quantum error-correcting code.
- Encoded gates are interspersed with non-destructive quantum error correction.
- Encoded gates and error correction operations are designed in a way that limits the *spread* of errors.

*“One failure should produce at most one error in any encoded qubit”*

# Excerpt from an encoded circuit



To satisfy the one-failure-one-error principle the encoded ancilla is *verified* against  $X$  errors.

## Encoded failures and thresholds

An encoded gate with error correction consists of  $C$  physical *locations* at which errors can occur. If the physical failure rate is  $\epsilon$ , and the quantum code can correct up to  $t$  errors, then a bound on the *encoded failure rate*  $\epsilon'$  is given by

$$\epsilon' < \binom{C}{t+1} \epsilon^{t+1}.$$

For a computation of  $m$  steps, we require  $\epsilon' \sim p/m$ , however larger  $t$  implies larger  $C$ , and for families of codes useful for encoded computation this requires  $\epsilon \sim O(1/\log^d(m))$ .

A final principle used to achieve constant thresholds is recursive encodings or *concatenation*, for which we have the *threshold condition*  $\epsilon' < \epsilon$  or

$$\epsilon < 1/\binom{C}{t+1}^{1/t}.$$

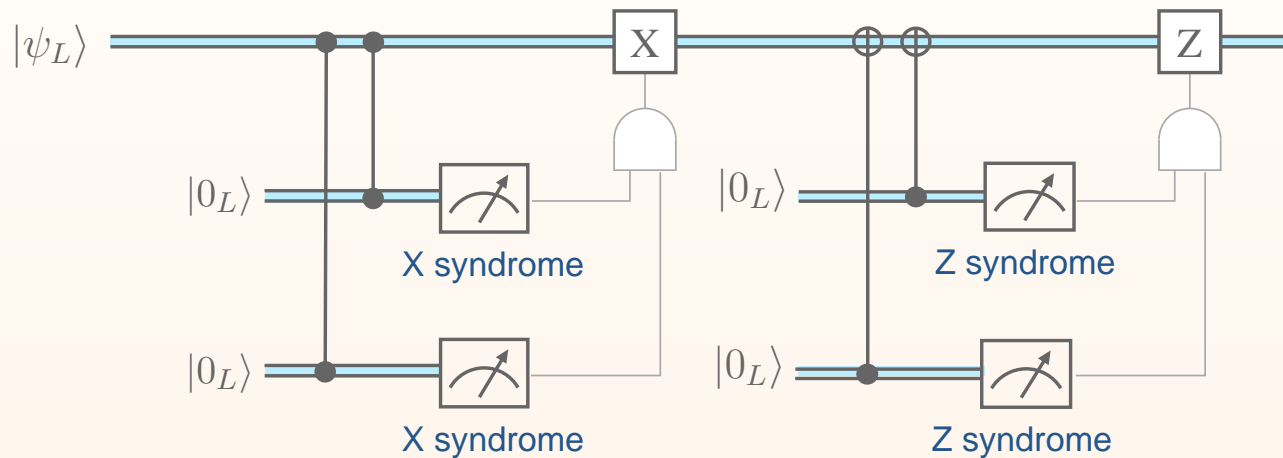
This is the content of the threshold theorem for asymptotically scalable quantum computation and provides a lower bound for the value of a threshold for a fault-tolerant architecture. In practice it is an overly pessimistic as

- No distinction between ‘benign’ and ‘malignant’ sets of error locations.
- Difficult to enumerate relevant locations in more sophisticated architectures

## Numerical and heuristic threshold estimates

More accurate estimates of the threshold for any architecture can be obtained via numerical and heuristic analysis.

For example:

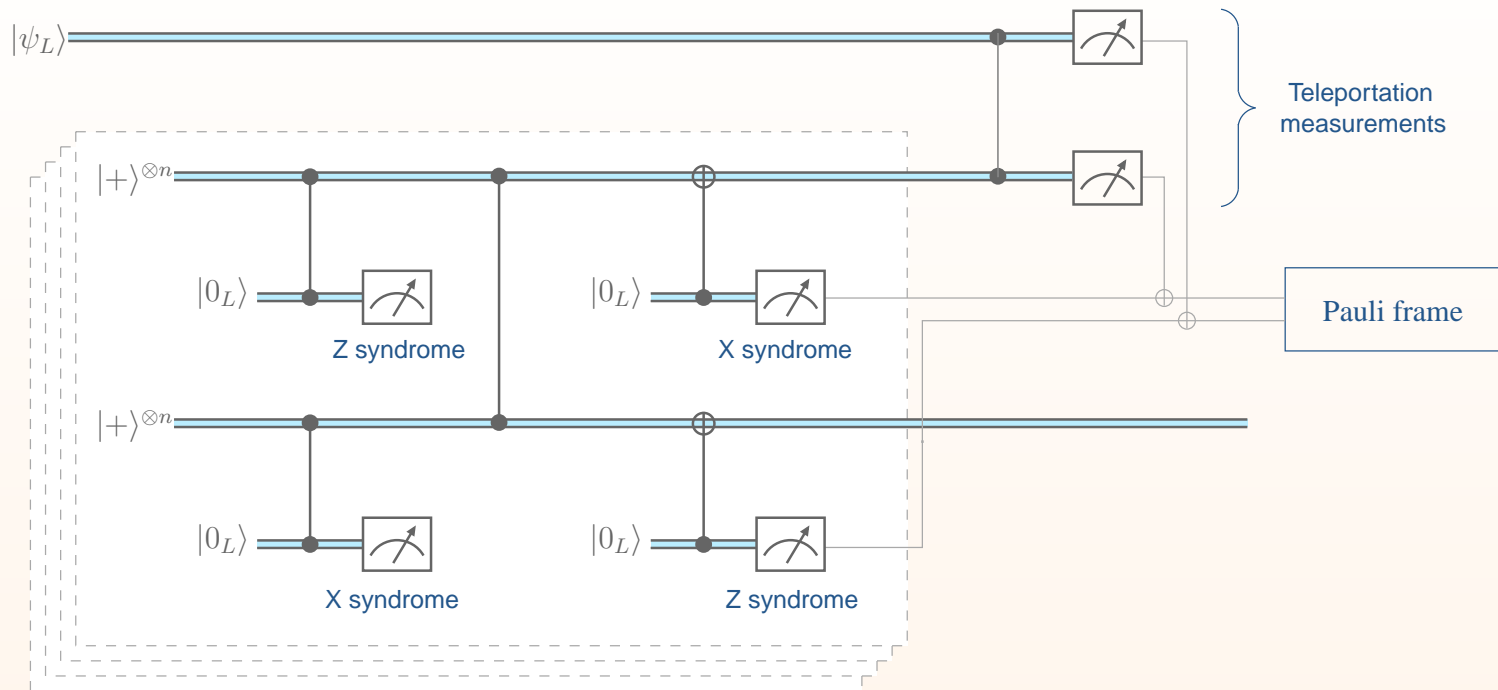


Steane  
Phys. Rev. A **68**,  
042322 (2003)

By confirming syndromes twice the likelihood of misdiagnosing an error and making things worse is reduced.

Steane numerically obtained a threshold of  $10^{-4}$  for the  $[[7, 1, 3]]$  code and uniform depolarization rates for gates, memory and measurement.

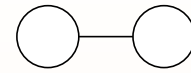
# Teleported error correction (Telecorrection)



- Repeated syndrome extractions performed ‘offline’ and postselected for agreement.
- Reduced operations on encoded data qubit.
- Natural loss detection and reduction to Pauli errors.
- Errors are not explicitly corrected — syndrome and teleportation measurement results are used to maintain a *Pauli frame* for each physical qubit’s computational basis.
- Numerically estimated threshold  $10^{-3}$  for  $[[7, 1, 3]]$  code and uniform depolarization rate. (c.f. Knill  $10^{-2}$ )

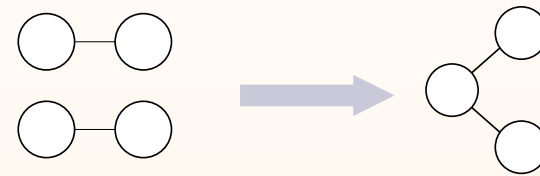
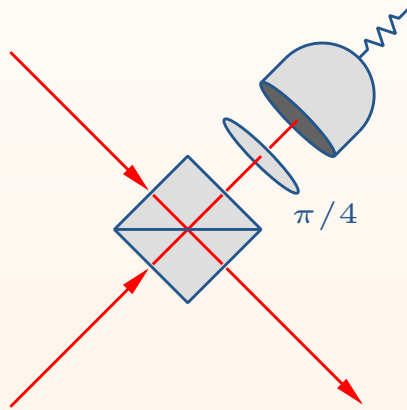
# Physical primitives of optical telecorrection

Source(s) of polarization encoded Bell pairs

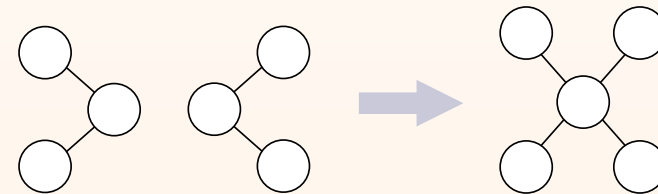


Linear optics and polarization discriminating photon counters (0, 1, 2+)

Optical fusion gates (Type-I)

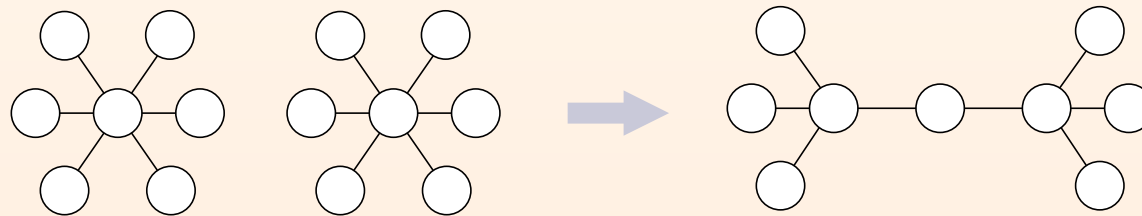


$$p_{\text{success}} = \frac{1}{2}$$



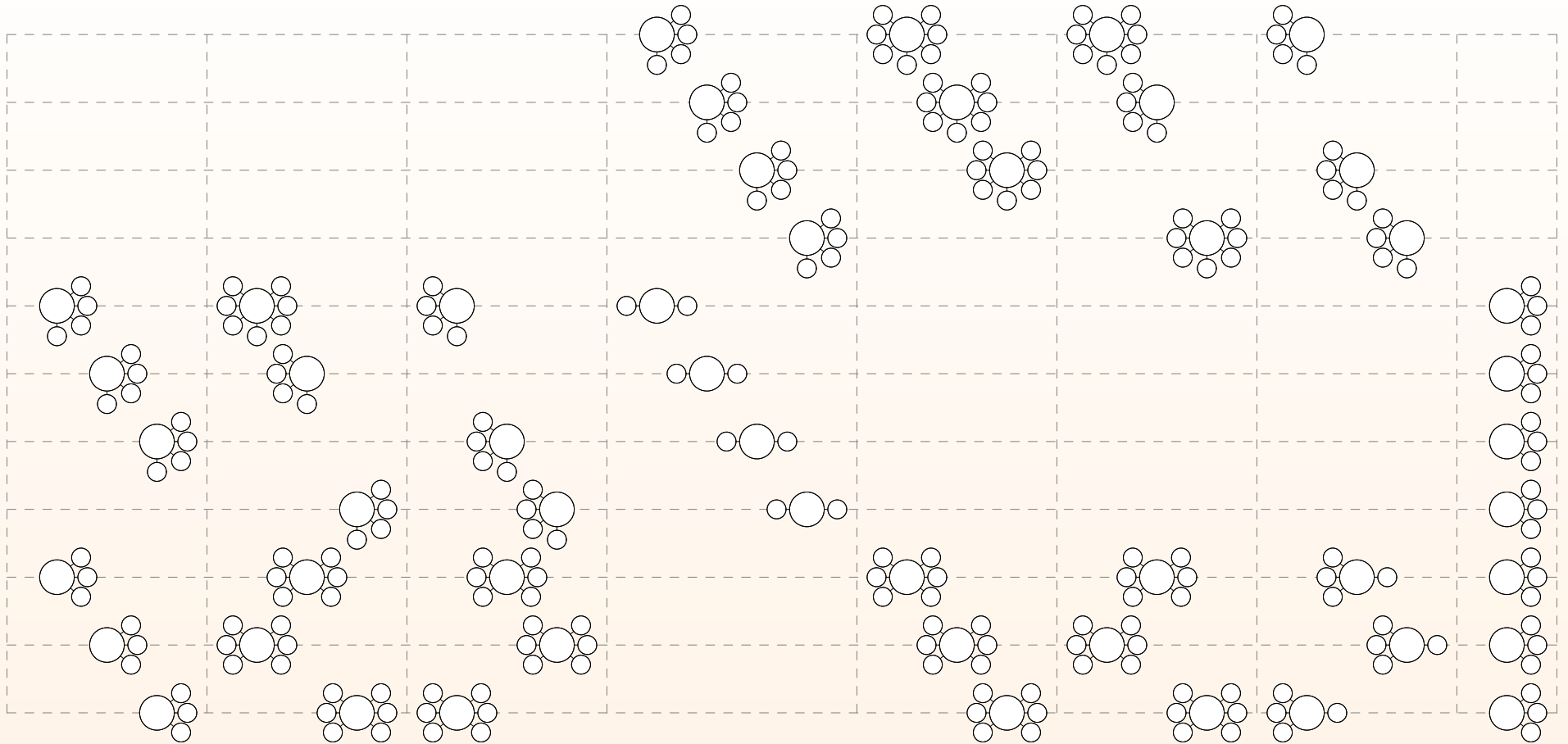
$$p_{\text{success}} = \frac{1}{2}$$

Star-shaped *microclusters* like this are used as building blocks for nearer-deterministic preparation of optical cluster states:

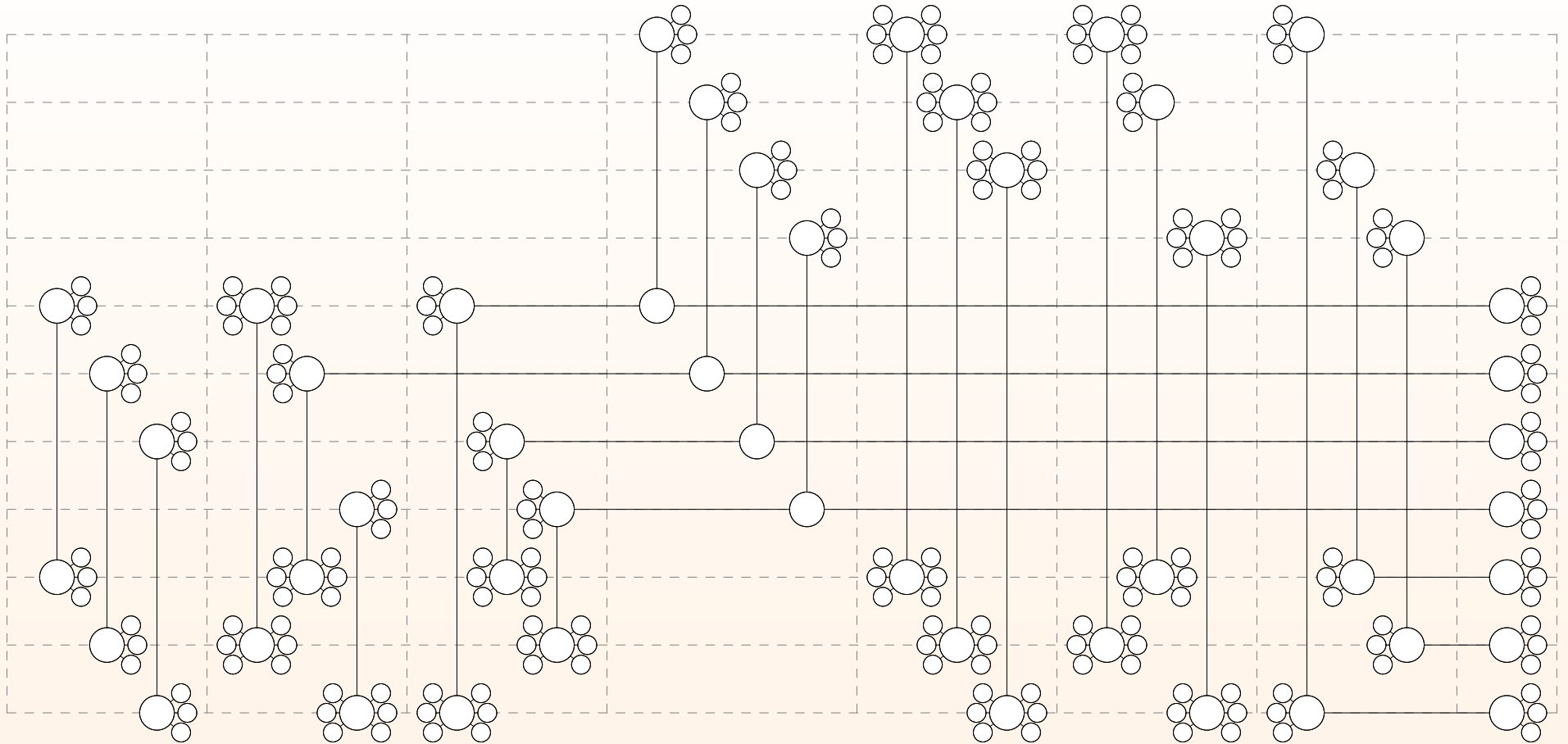


$$p_{\text{success}} = \frac{7}{8}$$

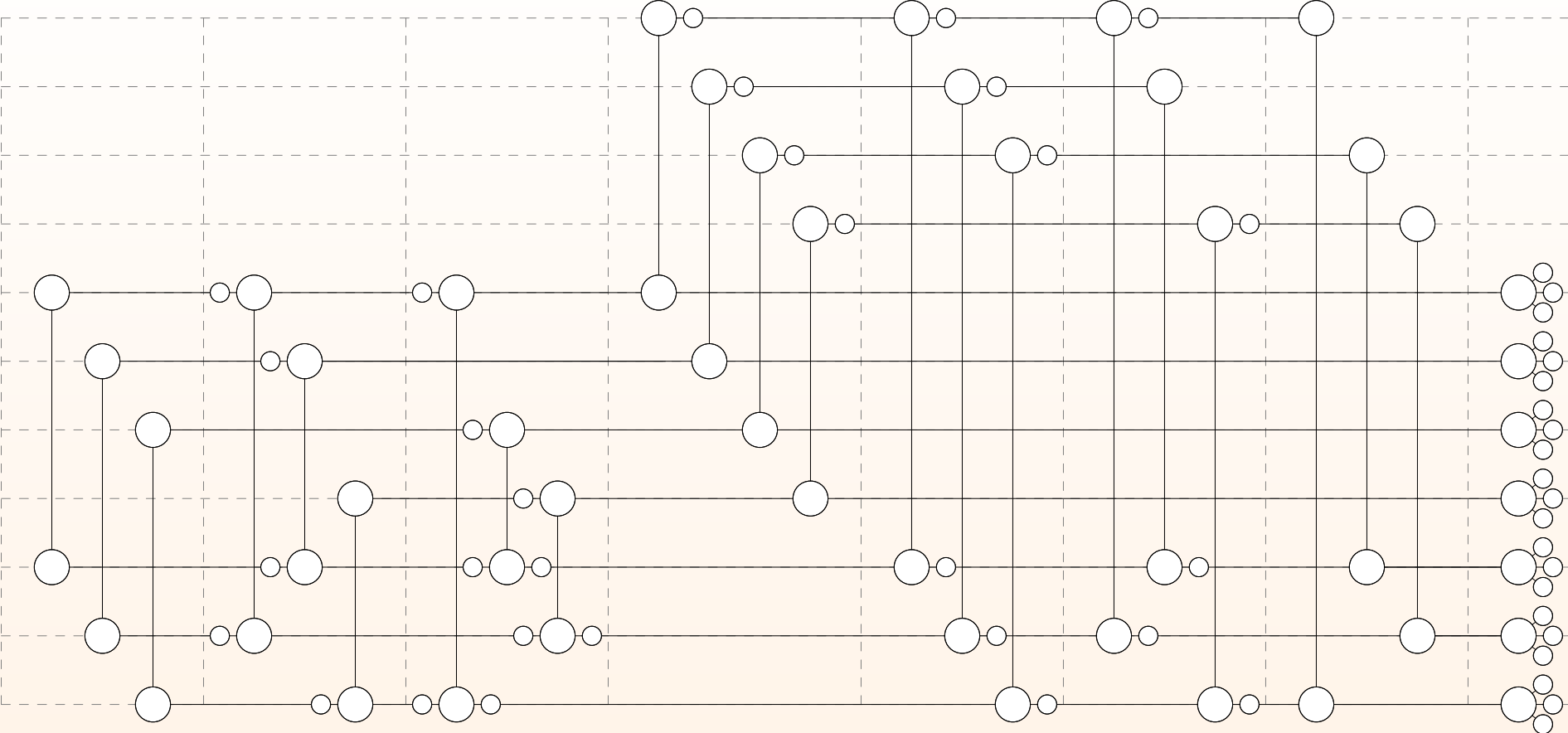
# e.g. Verified optical ancilla



# e.g. Verified optical ancilla



e.g. Verified optical ancilla

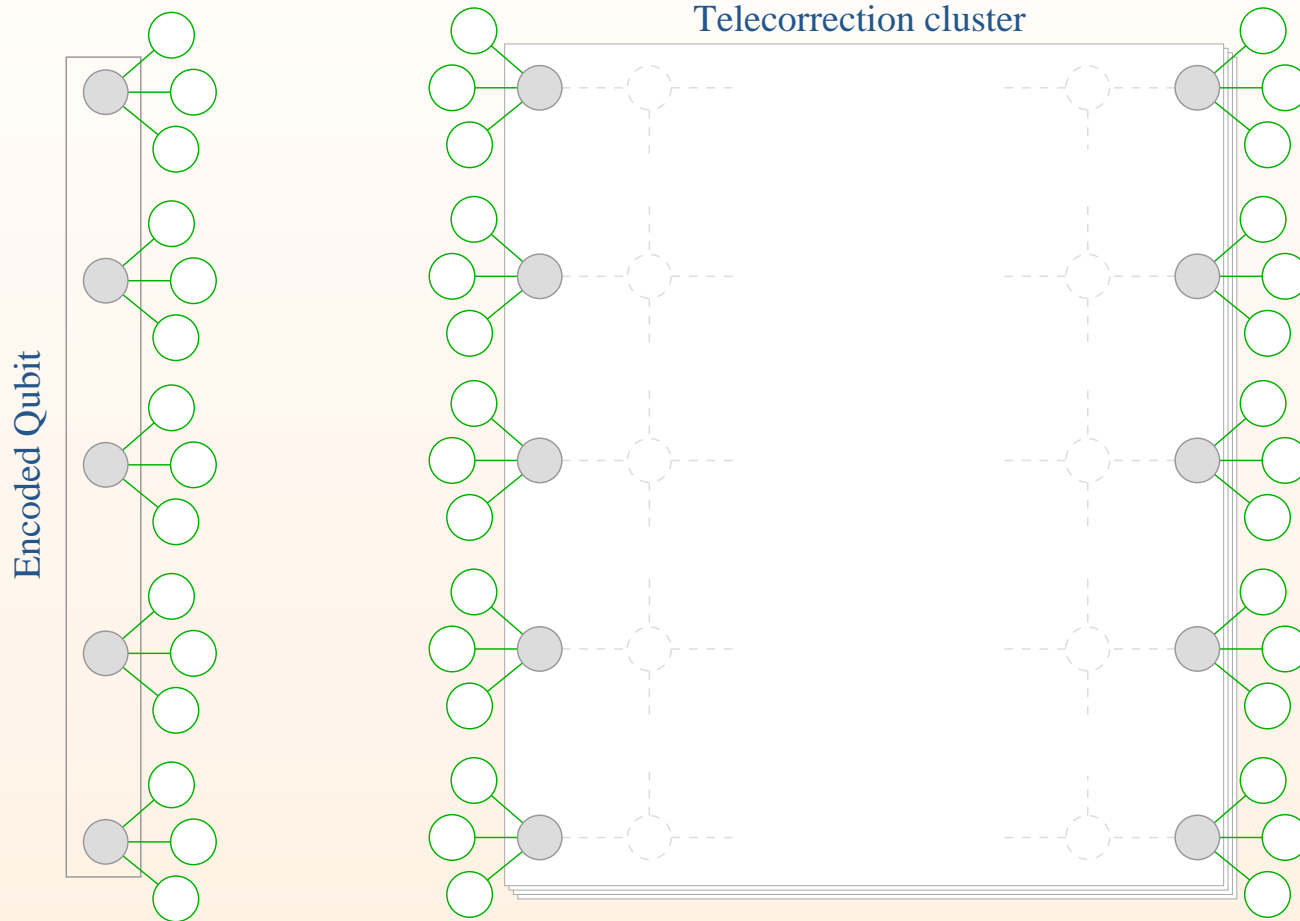


## Optical telecorrection

The teleported error correction protocol is implemented in the optical cluster-state model by preparing a *telecorrector* cluster that is post-selected for (a) non-determinism, (b) photon loss, and (c) pre-agreeing syndromes.

# Optical telecorrection

The teleported error correction protocol is implemented in the optical cluster-state model by preparing a *telecorrector* cluster that is post-selected for (a) non-determinism, (b) photon loss, and (c) pre-agreeing syndromes.

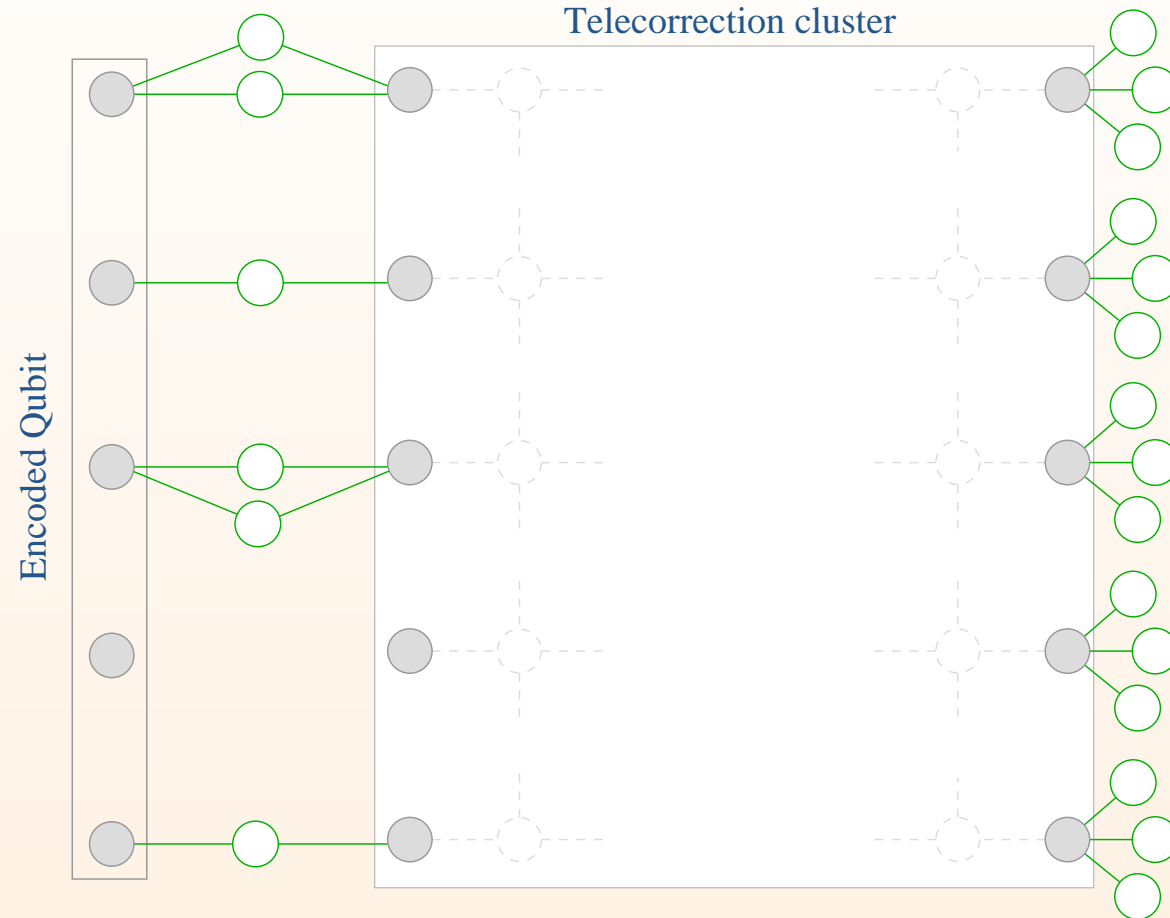


The unmeasured qubits are used for multiple attempts at fusing this cluster to the existing encoded data.

To finish the outputs of the fusions are measured as usual for cluster-state computation, and the Pauli frame updated to account for these and the telecorrection results.

# Optical telecorrection

The teleported error correction protocol is implemented in the optical cluster-state model by preparing a *telecorrector* cluster that is post-selected for (a) non-determinism, (b) photon loss, and (c) pre-agreeing syndromes.

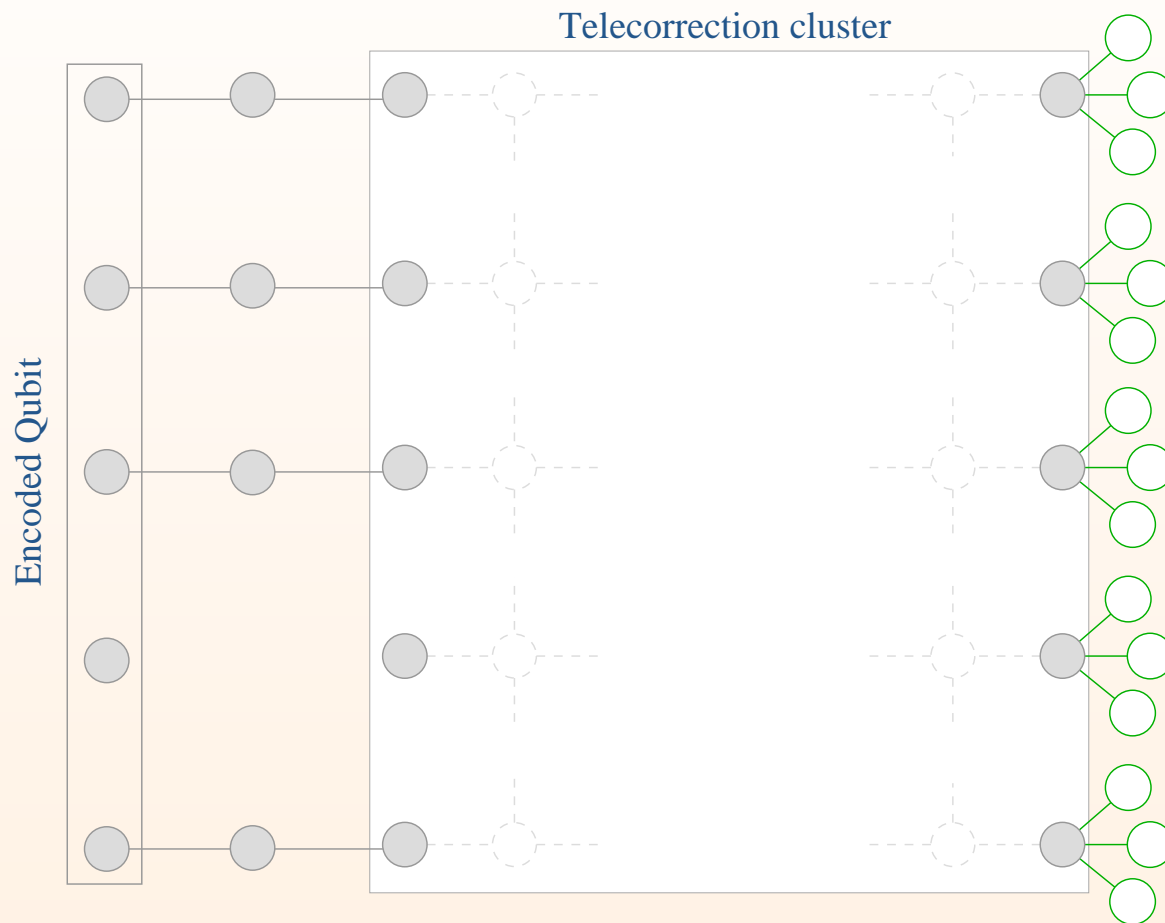


The unmeasured qubits are used for multiple attempts at fusing this cluster to the existing encoded data.

To finish the outputs of the fusions are measured as usual for cluster-state computation, and the Pauli frame updated to account for these and the telecorrection results.

# Optical telecorrection

The teleported error correction protocol is implemented in the optical cluster-state model by preparing a *telecorrector* cluster that is post-selected for (a) non-determinism, (b) photon loss, and (c) pre-agreeing syndromes.

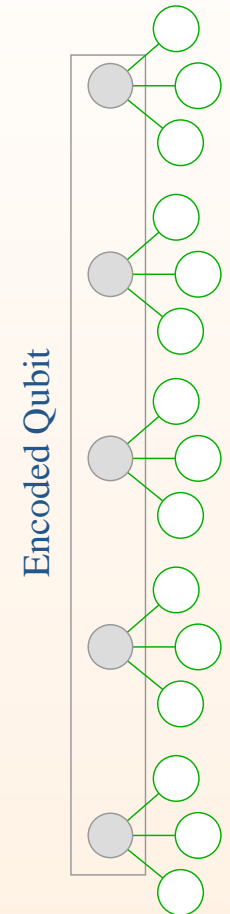


The unmeasured qubits are used for multiple attempts at fusing this cluster to the existing encoded data.

To finish the outputs of the fusions are measured as usual for cluster-state computation, and the Pauli frame updated to account for these and the telecorrection results.

# Optical telecorrection

The teleported error correction protocol is implemented in the optical cluster-state model by preparing a *telecorrector* cluster that is post-selected for (a) non-determinism, (b) photon loss, and (c) pre-agreeing syndromes.



The unmeasured qubits are used for multiple attempts at fusing this cluster to the existing encoded data.

To finish the outputs of the fusions are measured as usual for cluster-state computation, and the Pauli frame updated to account for these and the telecorrection results.

# Error model and threshold results

## Error model and threshold results

**Depolarization' errors** are assumed to occur independently on each Bell pairs preparation, fusion, memory step, and measurement with probability  $\epsilon$  (joint depolarization' on Bell pairs and fusion inputs).

## Error model and threshold results

**Depolarization errors** are assumed to occur independently on each Bell pairs preparation, fusion, memory step, and measurement with probability  $\epsilon$  (joint depolarization on Bell pairs and fusion inputs).

**Loss errors** are similarly assumed to affect each primitive with probability  $\gamma$ . The effect of a loss is simulated by randomizing the Pauli frame for that qubit. (Errors due to fusion failures are treated similarly).

## Error model and threshold results

**Depolarization' errors** are assumed to occur independently on each Bell pairs preparation, fusion, memory step, and measurement with probability  $\epsilon$  (joint depolarization' on Bell pairs and fusion inputs).

**Loss errors** are similarly assumed to affect each primitive with probability  $\gamma$ . The effect of a loss is simulated by randomizing the Pauli frame for that qubit. (Errors due to fusion failures are treated similarly).

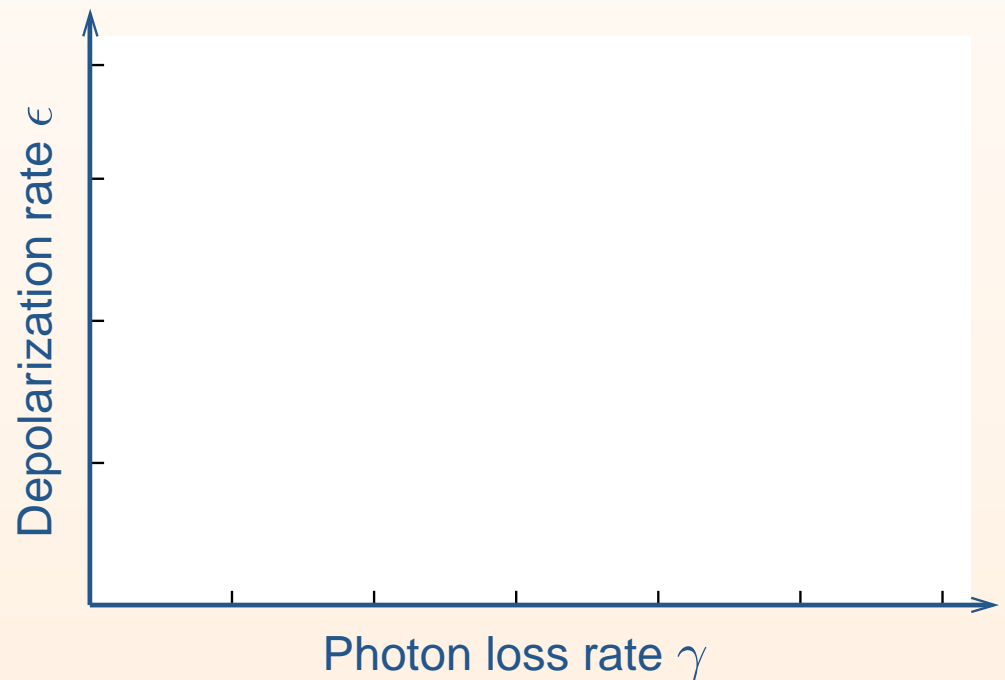
The performance of the optical architecture under this error model was determined by numerical simulation, providing estimates of *located* and *unlocated* encoded failure rates for a given  $\epsilon, \gamma$ .

## Error model and threshold results

**Depolarization errors** are assumed to occur independently on each Bell pairs preparation, fusion, memory step, and measurement with probability  $\epsilon$  (joint depolarization on Bell pairs and fusion inputs).

**Loss errors** are similarly assumed to affect each primitive with probability  $\gamma$ . The effect of a loss is simulated by randomizing the Pauli frame for that qubit. (Errors due to fusion failures are treated similarly).

The performance of the optical architecture under this error model was determined by numerical simulation, providing estimates of *located* and *unlocated* encoded failure rates for a given  $\epsilon, \gamma$ .

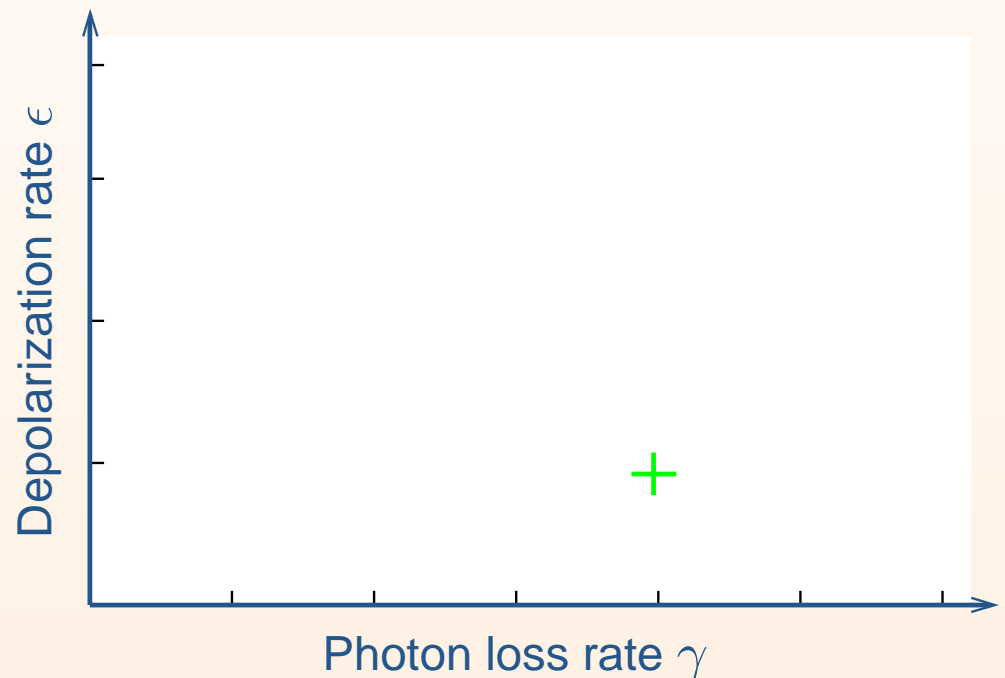


## Error model and threshold results

**Depolarization errors** are assumed to occur independently on each Bell pairs preparation, fusion, memory step, and measurement with probability  $\epsilon$  (joint depolarization on Bell pairs and fusion inputs).

**Loss errors** are similarly assumed to affect each primitive with probability  $\gamma$ . The effect of a loss is simulated by randomizing the Pauli frame for that qubit. (Errors due to fusion failures are treated similarly).

The performance of the optical architecture under this error model was determined by numerical simulation, providing estimates of *located* and *unlocated* encoded failure rates for a given  $\epsilon, \gamma$ .

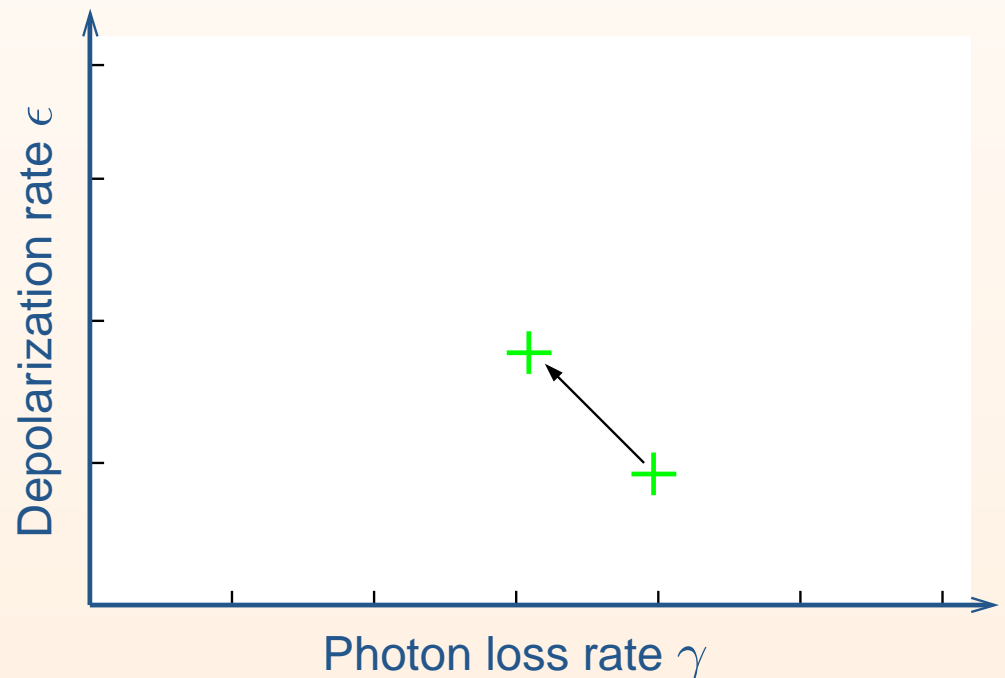


## Error model and threshold results

**Depolarization errors** are assumed to occur independently on each Bell pairs preparation, fusion, memory step, and measurement with probability  $\epsilon$  (joint depolarization on Bell pairs and fusion inputs).

**Loss errors** are similarly assumed to affect each primitive with probability  $\gamma$ . The effect of a loss is simulated by randomizing the Pauli frame for that qubit. (Errors due to fusion failures are treated similarly).

The performance of the optical architecture under this error model was determined by numerical simulation, providing estimates of *located* and *unlocated* encoded failure rates for a given  $\epsilon, \gamma$ .

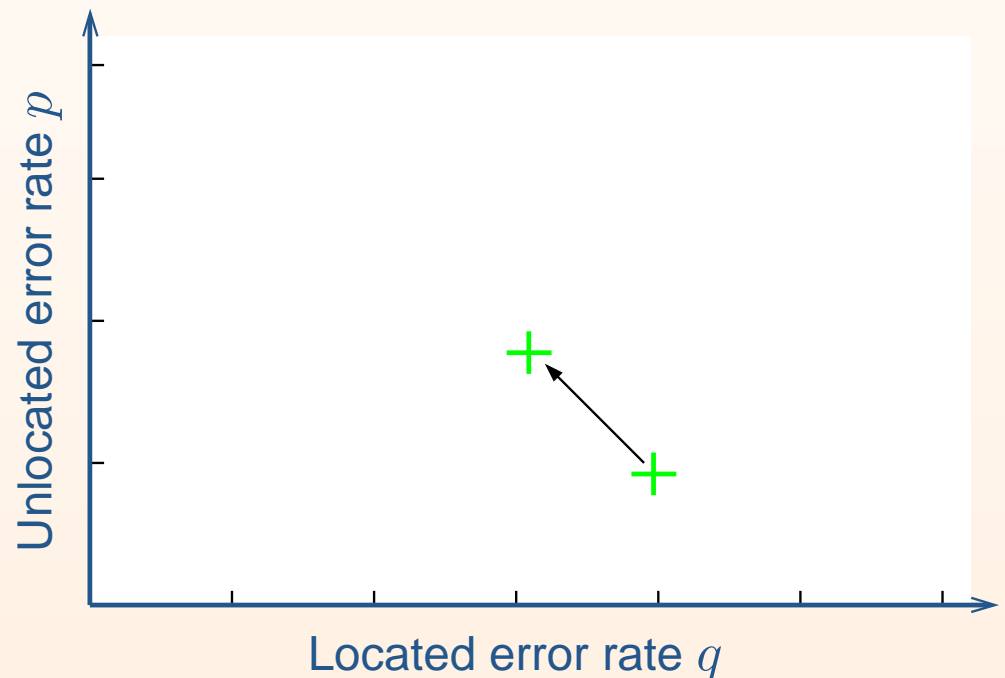


## Error model and threshold results

**Depolarization errors** are assumed to occur independently on each Bell pairs preparation, fusion, memory step, and measurement with probability  $\epsilon$  (joint depolarization on Bell pairs and fusion inputs).

**Loss errors** are similarly assumed to affect each primitive with probability  $\gamma$ . The effect of a loss is simulated by randomizing the Pauli frame for that qubit. (Errors due to fusion failures are treated similarly).

The performance of the optical architecture under this error model was determined by numerical simulation, providing estimates of *located* and *unlocated* encoded failure rates for a given  $\epsilon, \gamma$ .



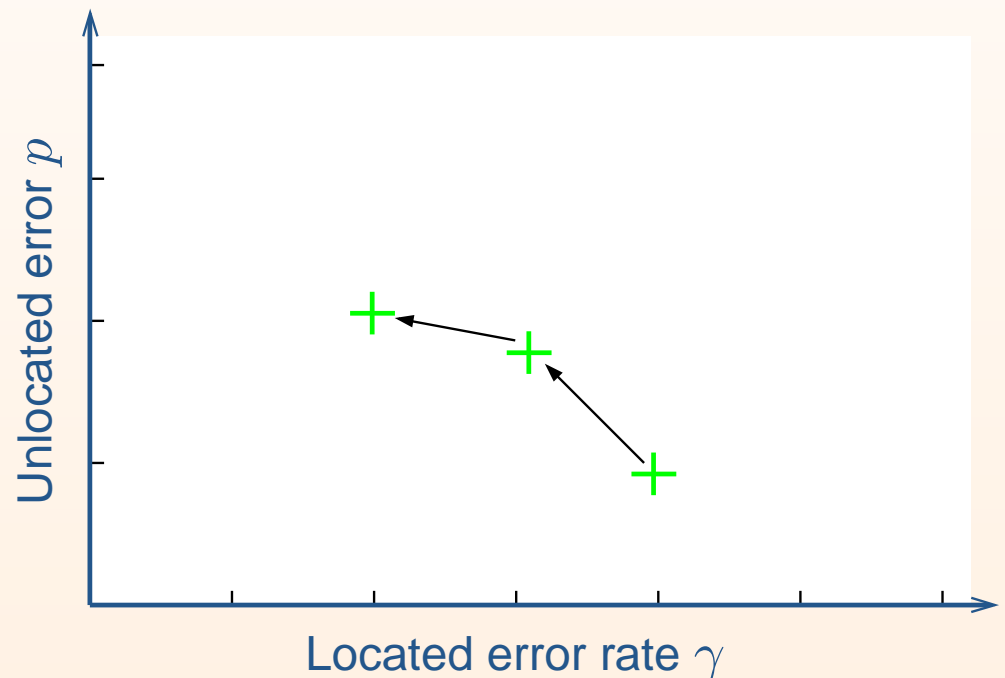
Higher levels of encoding are implemented with circuit model telecorrection.

## Error model and threshold results

**Depolarization errors** are assumed to occur independently on each Bell pairs preparation, fusion, memory step, and measurement with probability  $\epsilon$  (joint depolarization on Bell pairs and fusion inputs).

**Loss errors** are similarly assumed to affect each primitive with probability  $\gamma$ . The effect of a loss is simulated by randomizing the Pauli frame for that qubit. (Errors due to fusion failures are treated similarly).

The performance of the optical architecture under this error model was determined by numerical simulation, providing estimates of *located* and *unlocated* encoded failure rates for a given  $\epsilon, \gamma$ .



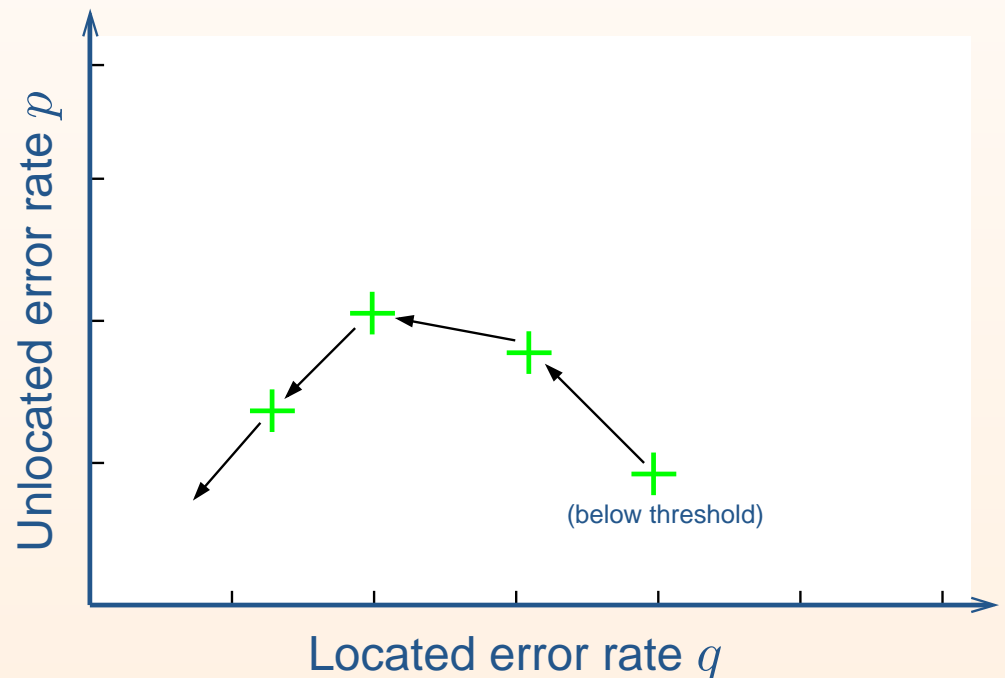
Higher levels of encoding are implemented with circuit model telecorrection.

## Error model and threshold results

**Depolarization errors** are assumed to occur independently on each Bell pairs preparation, fusion, memory step, and measurement with probability  $\epsilon$  (joint depolarization on Bell pairs and fusion inputs).

**Loss errors** are similarly assumed to affect each primitive with probability  $\gamma$ . The effect of a loss is simulated by randomizing the Pauli frame for that qubit. (Errors due to fusion failures are treated similarly).

The performance of the optical architecture under this error model was determined by numerical simulation, providing estimates of *located* and *unlocated* encoded failure rates for a given  $\epsilon, \gamma$ .



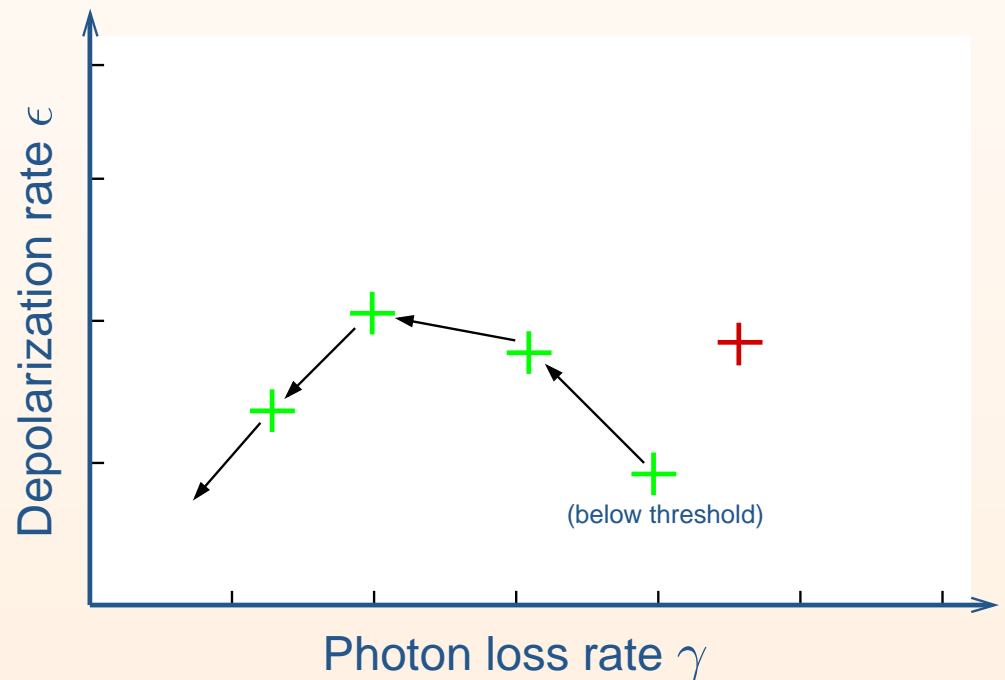
Higher levels of encoding are implemented with circuit model telecorrection.

## Error model and threshold results

**Depolarization errors** are assumed to occur independently on each Bell pairs preparation, fusion, memory step, and measurement with probability  $\epsilon$  (joint depolarization on Bell pairs and fusion inputs).

**Loss errors** are similarly assumed to affect each primitive with probability  $\gamma$ . The effect of a loss is simulated by randomizing the Pauli frame for that qubit. (Errors due to fusion failures are treated similarly).

The performance of the optical architecture under this error model was determined by numerical simulation, providing estimates of *located* and *unlocated* encoded failure rates for a given  $\epsilon, \gamma$ .



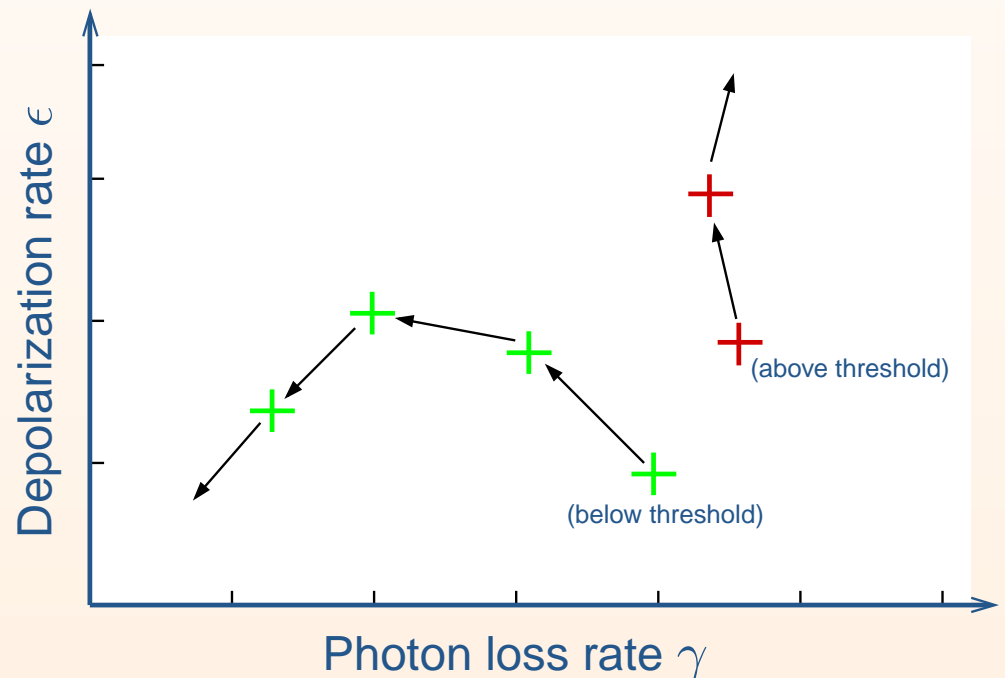
Higher levels of encoding are implemented with circuit model telecorrection.

## Error model and threshold results

**Depolarization errors** are assumed to occur independently on each Bell pairs preparation, fusion, memory step, and measurement with probability  $\epsilon$  (joint depolarization on Bell pairs and fusion inputs).

**Loss errors** are similarly assumed to affect each primitive with probability  $\gamma$ . The effect of a loss is simulated by randomizing the Pauli frame for that qubit. (Errors due to fusion failures are treated similarly).

The performance of the optical architecture under this error model was determined by numerical simulation, providing estimates of *located* and *unlocated* encoded failure rates for a given  $\epsilon, \gamma$ .



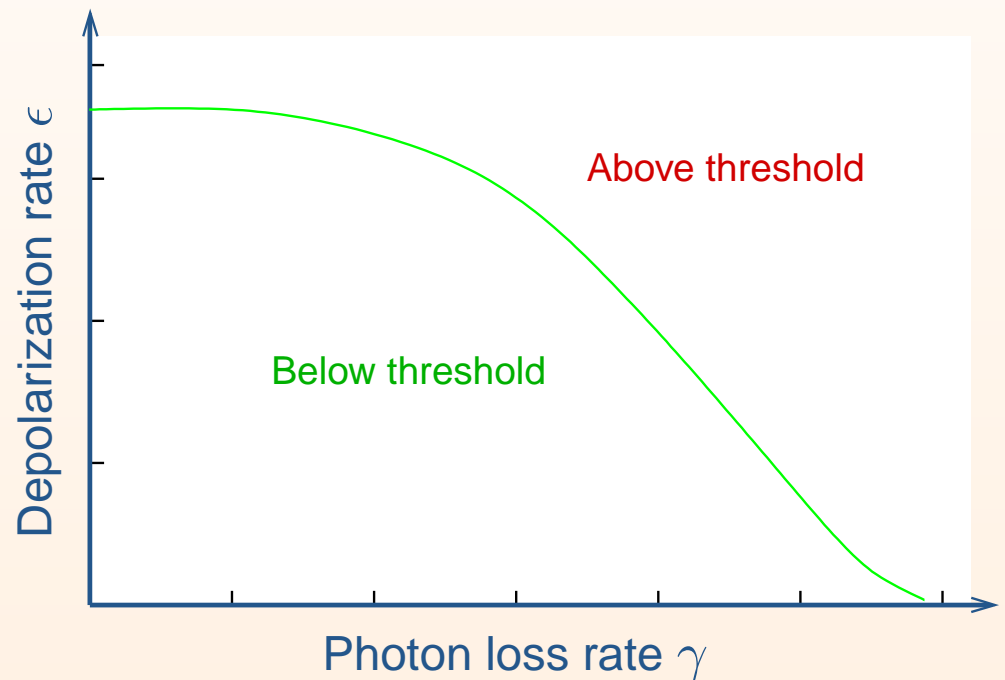
Higher levels of encoding are implemented with circuit model telecorrection.

## Error model and threshold results

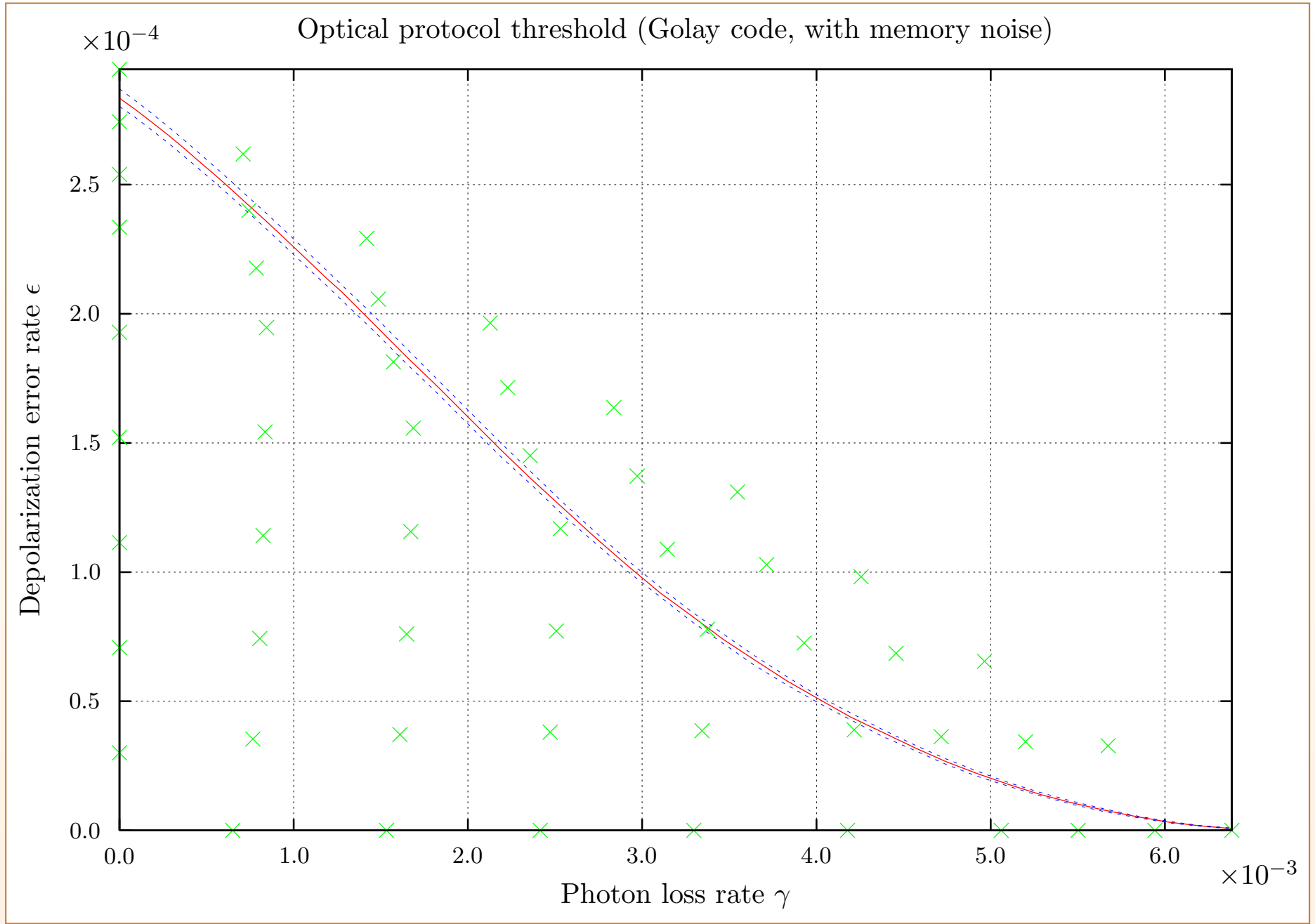
**Depolarization errors** are assumed to occur independently on each Bell pairs preparation, fusion, memory step, and measurement with probability  $\epsilon$  (joint depolarization on Bell pairs and fusion inputs).

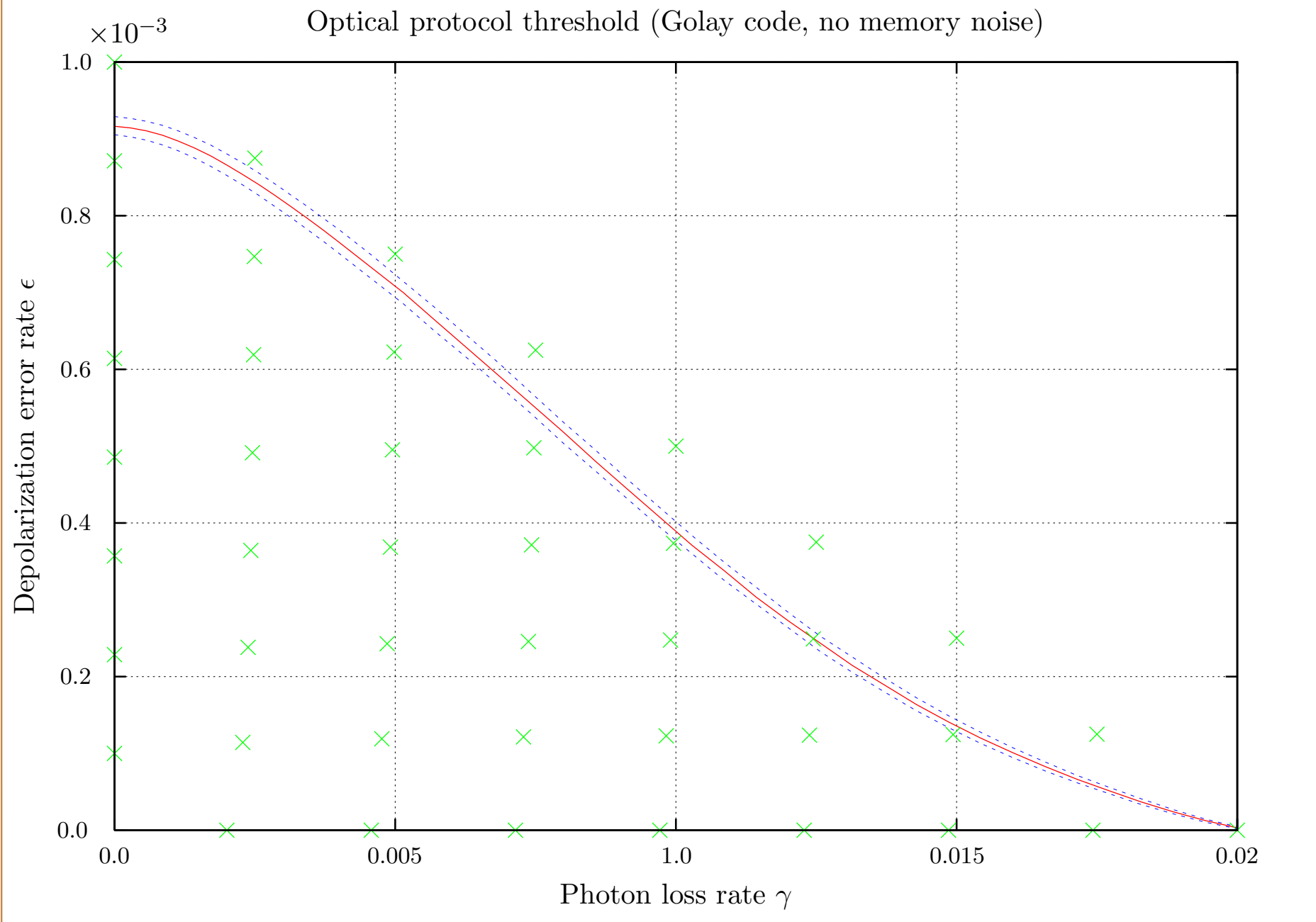
**Loss errors** are similarly assumed to affect each primitive with probability  $\gamma$ . The effect of a loss is simulated by randomizing the Pauli frame for that qubit. (Errors due to fusion failures are treated similarly).

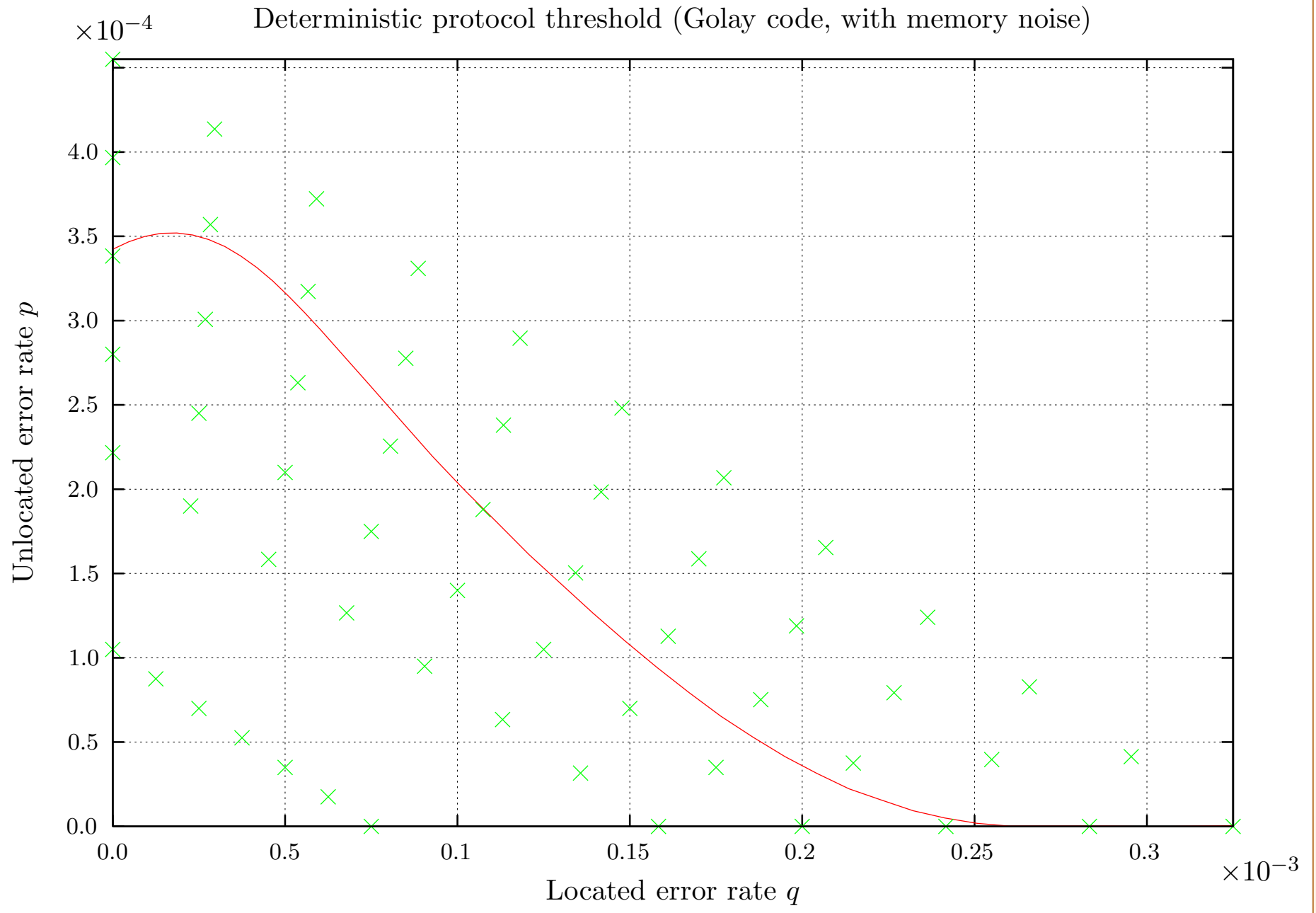
The performance of the optical architecture under this error model was determined by numerical simulation, providing estimates of *located* and *unlocated* encoded failure rates for a given  $\epsilon, \gamma$ .



Higher levels of encoding are implemented with circuit model telecorrection.







## Conclusions and outlook

Fault-tolerant architectures make use of scale to deal with problems introduced by scale. In principle, remarkably high thresholds are possible.

**Caveat:** The resources required for to achieve such resources can be imposing. The telecorrector cluster state shown earlier requires on average  $\approx 62$  million Bell pairs for its (badly unoptimized) non-deterministic preparation.

### **Reasons for optimism:**

- Ample scope for optimizations to preparation of telecorrection media.
- An optical architecture based on Knill's telecorrection protocol<sup>1</sup> would easily improve this. There are also more efficient cluster-state preparation schemes<sup>2</sup>
- Substantial improvements to thresholds are likely by exploiting the 'good' physical primitives.
- Smaller quantum computations and simulations may be implementable without encoding.

---

<sup>1</sup>E. Knill, *Nature* **434**, 39–44 2005

<sup>2</sup>Kieling et al. arXiv:quant-ph/0601190

## 1952 IBM vacuum tube logic kit



### 1955 classical fault-tolerance<sup>3</sup> for an error rate of 0.005

Consider a computing machine with 2500 vacuum tubes, each of which is actuated on the average once every 5 microseconds. Assume a mean free path of 8 hours between errors is desired. In this period there will have been  $1/5 \times 2,500 \times 8 \times 3,600 \times 10^6 = 1.4 \times 10^{13}$  actuations, hence the above specification calls for an effective error rate of  $1/[1.4 \times 10^{13}] = 7 \times 10^{14}$ . From the above table this calls for  $N$  between 10,000 and 20,000 -- interpolating loglinearly gives  $N = 14,000$  i.e. the system should be multiplexed 14,000 times.

<sup>3</sup>J. von Neumann, in Automata Studies, Princeton University Press, 1956.